OPEN

Immunomics of Renal Allograft Acute T Cell-Mediated Rejection Biopsies of Tacrolimus- and Belatacept-Treated Patients

Marieke van der Zwan, MD,[1] Carla C. Baan, PhD,[1] Robert B. Colvin, MD, PhD,[2] Rex N. Smith, MD, PhD,[2] Rebecca A. White,[2] Dorothy Ndishabandi,[2] Alex L. Nigg,[3] Thierry P.P. van den Bosch, PhD,[3] Gretchen N. de Graav, MD, PhD,[1] Marian C. Clahsen-van Groningen, MD, PhD,[3] and Dennis A. Hesselink, MD, PhD[1]

Background. Belatacept-based therapy in kidney transplant recipient has been shown to increase long-term renal allograft and patient survival compared with calcineurin inhibitor–based therapy, however, with an increased risk of acute T cell-mediated rejection (aTCMR). An improved understanding of costimulation blockade-resistant rejections could lead to a more personalized approach to belatacept therapy. Here, immunomic profiles of aTCMR biopsies of patients treated with either tacrolimus or belatacept were compared. **Methods.** Formalin-fixed paraffin-embedded renal transplant biopsies were used for immunohistochemistry and gene expression analysis using the innovative NanoString technique. To validate NanoString, transcriptomic profiles of patients with and without biopsy-proven aTCMR were compared. Biopsies from 31 patients were studied: 14 tacrolimus-treated patients with aTCMR, 11 belatacept-treated patients with aTCMR, and 6 controls without rejection. **Results.** A distinct pattern was seen in biopsies with aTCMR compared to negative controls: 78 genes had a higher expression in the aTCMR group (false discovery rate *P* value <.05 to 1.42e–05). The most significant were T cell-associated genes (CD3, CD8, and CD4; $P < 1.98e-04$), γ-interferon-inducible genes (CCL5, CXCL9, CXCL11, CXCL10, TBX21; $P < 1.33e-04$) plus effector genes (GNLY, GZMB, ITGAX; $P < 2.82e-03$). Immunophenotypical analysis of the classic immune markers of the innate and adaptive immune system was comparable between patients treated with either tacrolimus or belatacept. In addition, the transcriptome of both groups was not significantly different. **Conclusions.** In this small pilot study, no difference was found in immunomics of aTCMR biopsies of tacrolimus- and belatacept-treated patients. This suggests that clinically diagnosed aTCMR reflects a final common pathway of allorecognition which is unaffected by the type of immunosuppressive therapy.

(*Transplantation Direct* 2018;4: e418; doi: 10.1097/TXD.0000000000000857. Published online 20 December, 2018.)

Gene expression analysis of the kidney transplant biopsy has been shown to improve classification and risk stratification of patients when used in combination with current diagnostic standards.[1] The "molecular microscope" has been postulated to give a better insight into the

Received 1 November 2018. Revision requested 2 November 2018.

Accepted 10 November 2018.

[1] *Department of Internal Medicine, Division of Nephrology and Transplantation, Rotterdam Transplant Group, Erasmus MC, Rotterdam, the Netherlands.*

[2] *Department of Pathology, Massachusetts General Hospital/Harvard Medical School, Boston, MA.*

[3] *Department of Pathology, Erasmus MC, Rotterdam, the Netherlands.*

M.C.C.-v.G. and D.A.H. contributed equally to the writing of this article.

D.A.H. has received grant support from Astellas Pharma and Bristol Myers-Squibb, and has received lecture and consulting fees from Astellas Pharma and Chiesi Pharma. The other authors declare no conflicts of interest.

No sources of funding were used in the preparation of this article.

M.v.d.Z. participated in the research design, acquisition of the data, data analysis and writing of the article. R.B.C. and R.N.S participated in the research design, acquisition of the data and critical revision of the article. R.A.W., N.D., A.L.N., T.P.P.v.d.B. and G.N.d.G. participated in the acquisition of the data. C.C.B. and D.A.H. and participated in the research design, data analysis and critical revision of the article. M.C.C-v.G. participated in the research design, revision of the Banff classification of the kidney biopsies, data analysis, and critical revision of the article.

Correspondence: M. van der Zwan, MD, Department of Internal Medicine, Division of Nephrology and Kidney Transplantation, Rotterdam Transplant Group, Erasmus MC, University Medical Center Rotterdam, Rm Na-522, P.O. Box 2040, 3000 CA Rotterdam, The Netherlands. (m.vanderzwan@erasmusmc.nl).

Supplemental digital content (SDC) is available for this article. Direct URL citations appear in the printed text, and links to the digital files are provided in the HTML text of this article on the journal's Web site (www.transplantationdirect.com).

ISSN: 2373-8731

DOI: 10.1097/TXD.0000000000000857

classification of renal transplant pathology.[1-4] With the use of both gene and protein expression analysis, also known as immunomics, more insight can be gained in the pathophysiology of inflammatory reactions in the renal allograft.

The Banff guideline is a pathology-based classification system to diagnose acute renal transplant rejection.[5] However, this classification is vulnerable to misinterpretation and the Banff 2017 guideline states that the combination of conventional histomorphologic examination of a kidney transplant biopsy with molecular diagnostics leads to superior diagnostic classification and has the potential to guide therapy and improve allograft outcomes.[5,6] The novel technique NanoString allows for multiplex messenger RNA (mRNA) analysis of minute quantities of mRNA from formalin-fixed, paraffin-embedded (FFPE) biopsies without the need of preamplification.[2] With this technique, residual material from conventional histopathological diagnosis can be analyzed.[7,8] NanoString makes it possible to render data on the intragraft gene expression of up to 770 targets of interest within 2 days and with a comparable sensitivity to quantitative real-time polymerase chain reaction, and a better sensitivity than microarray.[8,9]

Long-term outcomes of kidney transplantation are negatively influenced by the nephrotoxicity and metabolic side effects of calcineurin inhibitor–based therapy.[10,11] A calcineurin inhibitor–free immunosuppressive regimen with the costimulation blocking drug belatacept has been shown to increase long-term renal allograft and patient survival.[12-14] However, belatacept-based immunosuppressive therapy is associated with an increased risk of acute T cell-mediated rejection (aTCMR).[15-18] Identification of factors that underlie such costimulation blockade-resistant rejection could lead to a more personalized approach to belatacept-based treatment through the identification of patients at "low risk" for acute rejection.[15,19-21]

To expand the understanding of the pathogenesis of costimulation blockade-resistant rejections, we have compared the immunomic profiles of aTCMR biopsies of patients treated with maintenance therapy consisting of either tacrolimus or belatacept. Gene expression analysis of 209 genes with the innovative NanoString technique in combination with immunohistochemistry (IHC) was used. To validate NanoString for our research question, transcriptomic profiles of patients with and without biopsy-proven aTCMR were compared.

MATERIALS AND METHODS

Study Population and Materials

Renal allograft biopsies were obtained from kidney transplant recipients who previously participated in 1 of 2 prospective randomized controlled trials (RCT) (a belatacept study and a tacrolimus-dosing study) performed at the Erasmus MC, the Netherlands (see below). The design and results of these trials were published previously.[20,22] Both studies were approved by the institutional review board of Erasmus MC (Medical Ethical Review Board numbers 2010-080 and 2012-421). Eleven belatacept-treated patients experienced an aTCMR[20] and the renal allograft biopsies of these patients were analyzed here. These biopsies were compared with 14 biopsies of tacrolimus-treated patients with an aTCMR that were included in 1 of these 2 RCTs.[20,22] The biopsies were all for-cause biopsies that were matched for time after transplantation, Banff 2015 category and grade, and age of the recipient (Table 1). All biopsies were scored independently by 2 pathologists according to the Banff 2015 classification.[23] In case of differences in classification, consensus was met. Six renal transplant biopsies without histomorphologic changes (Banff category 1) were included as negative controls and these were either derived from one of the RCTs[20] or from the archives of the department of pathology of the Erasmus MC (Table 1). The negative controls were matched for age of the recipient and time after transplantation.

The patients who participated in the belatacept study were randomized to a belatacept- or tacrolimus-based immunosuppressive regimen, as described previously.[20] The main objective of the tacrolimus-dosing study was to examine whether a *CYP3A5* genotype-based tacrolimus starting dose leads to earlier achievement of the tacrolimus target predose concentration.[22] The target predose concentration of tacrolimus and the dosing of mycophenolate mofetil and glucocorticoids were identical in both RCTs.[20,22]

Histochemical and Immunohistochemical Stainings and Digital Quantification

Two-micron sections of FFPE renal allograft biopsies were stained with hematoxylin and eosin, Periodic acid–Schiff–diastase, and Jones' silver stain according to standard diagnostic practice. Subsequently, IHC stainings were performed on 4 μm FFPE cut sections with an automated, validated and accredited staining system (Ventana Benchmark ULTRA; Ventana Medical Systems, Tucson, AZ) using ultraview or optiview universal DAB detection Kit. Antibodies used (CD3, CD4, CD8, CD20, CD56, CD68, PD-1, and granzyme B) and dilutions are summarized in **Table S1, SDC** (http://links.lww.com/TXD/A156). FoxP3/CD4 staining was performed at MGH/Harvard, (Boston, MA). All sections were scanned at 40× magnification using Nanozoomer XR digital slide scanner (Hamamatsu, Hamamatsu City, Japan). Digital image analysis was performed using Visiopharm integrator system (Version 2017.2.4.3387) with Author module (Visiopharm, Hoersholm, Denmark). For each section, manual selection of only cortical tissue was made, excluding the medulla, artifacts, and the lumen of blood vessels larger than glomeruli. Image analysis Application Protocol Packages were developed to measure the total tissue area (μm^2) and the area percentage of positive staining.

RNA Extraction

Three consecutive 20-μm sections cut from each FFPE block were immediately transferred to sterile microcentrifuge tubes and stored at room temperature. Microtome blades were then replaced, and equipment sterilization was performed with RNase AWAY (Life Technologies, Carlsbad, CA) between blocks. Xylene deparaffinization and RNA extraction of the curls were performed with use of the Recover All Total Nucleic Acid Isolation Kit for FFPE (Life Technologies). RNA concentration and purity were measured with the Nano-Drop 2000 spectrophotometer (Thermo Fisher Scientific, Waltham, MA).

NanoString nCounter Assay, Data Normalization, and Analysis

A custom code set of 216 genes was created: 209 genes that are known to be involved in renal allograft rejection

TABLE 1.

Patient characteristics

Biopsy	Primary kidney disease	Age	Sex	Therapy	HLA MM[a]	Type tx	Preemptive[b]	Timing[c]	Pathology diagnosis	DSA[d]	eGFR	Used for IHC	Used for nanostring
1	Membranous glomerulopathy	71	M	Tac	2-2-1	LUR	No	152	aTCMR IB	Negative	16	Yes	Yes
2	Hypertension	73	M	Tac	2-1-2	LUR	Yes	82	aTCMR IB	Not tested	40	Yes	Yes
3	Hypertension	46	F	Tac	2-0-1	LUR	No	5	aTCMR IIA	Not tested	41	Yes	No
4	DM2	64	M	Tac	1-2-2	LUR	No	34	aTCMR IIA	Not tested	24	Yes	No
5	ADPKD	73	F	Tac	1-2-1	LUR	Yes	68	aTCMR IIA	Not tested	30	Yes	No
6	DM1	60	M	Tac	1-1-1	LR	Yes	91	aTCMR IIA	Not tested	35	Yes	No
7	Hypertension and DM2	76	M	Tac	2-2-1	LUR	Yes	10	aTCMR IIA	Negative	18	Yes	No
8	Unknown	56	F	Tac	2-2-2	LR	Yes	6	aTCMR IIA and AMR	Negative	28	Yes	Yes
9	Hypertension	46	F	Tac	1-2-1	LUR	No	9	aTCMR IIA and AMR	Negative	DGF	Yes	No
10	DM2	65	M	Tac	1-1-1	LUR	Yes	9	aTCMR IIB	Not tested	8	Yes	Yes
11	Urate nephropathy	55	F	Tac	1-1-1	LR	No	6	aTCMR IIB	Not tested	14	Yes	Yes
12	Alport syndrome	34	M	Tac	1-2-1	LUR	No	2	aTCMR IIB	Positive	DGF	Yes	Yes
13	Unknown	50	M	Tac	2-1-2	LUR	No	8	aTCMR IIB	Not tested	34	Yes	Yes
14	Hypertension	55	M	Tac	0-2-2	LUR	No	48	aTCMR IIB	Not tested	12	Yes	No
15	Unknown	26	M	Bela	1-1-1	LR	No	94	aTCMR IIB	Negative	56	Yes	Yes
16	ADPKD	66	F	Bela	1-2-1	LUR	Yes	70	aTCMR IIB	Negative	25	Yes	Yes
17	ATN after sepsis	76	M	Bela	1-2-1	LUR	No	13	aTCMR IIA and AMR	Negative	18	Yes	Yes
18	Nephrotoxicity chemotherapy	46	M	Bela	0-1-1	LR	Yes	64	aTCMR IIA	Negative	72	Yes	Yes
19	VUR	46	M	Bela	0-1-1	LR	Yes	44	aTCMR IIA	Negative	36	Yes	Yes
20	Hypertension and DM2	69	M	Bela	2-1-1	LUR	Yes	120	aTCMR IIB	Negative	27	Yes	Yes
21	Unknown	46	M	Bela	2-1-2	LUR	Yes	112	aTCMR IIB	Negative	28	Yes	Yes
22	Urologic	45	M	Bela	1-2-1	LUR	Yes	3	aTCMR IIB	Negative	16	Yes	Yes
23	GPA	28	F	Bela	1-1-1	LR	No	5	aTCMR IIB	Negative	34	Yes	No
24	ADPKD	48	F	Bela	1-1-1	LUR	No	4	aTCMR IIB and AMR	Negative	DGF	Yes	Yes
25	Unknown	62	F	Bela	1-2-2	LUR	Yes	56	aTCMR III	Negative	5	Yes	Yes
26	ADPKD	42	F	Tac	1-1-0	LR	Yes	28	Reactive changes (Banff cat. 1)	Not tested	45	No	Yes
27	ADPKD	61	M	Tac	1-1-1	LUR	No	31	Reactive changes (Banff cat. 1)	Not tested	37	No	Yes
28	Unknown	69	M	Tac	0-1-1	LR	No	13	Some infiltration in interstitium with eosinophil granulocytes (Banff cat. 1)	Not tested	58	No	Yes
29	GPA	27	M	Tac	0-0-0	LR	Yes	77	Arteriosclerosis, small area interstitial fibrosis (Banff cat. 1)	Not tested	63	No	Yes
30	Systemic lupus erythematosus	35	F	Tac	0-1-2	LUR	Yes	72	Arteriosclerosis, 10% IF/TA, some glomerular ischemia (Banff cat.1)	Not tested	33	No	Yes
31	Nephrotoxicity chemotherapy	45	M	Bela	0-1-1	LR	Yes	101	Intima fibrosis (Banff cat.1)	Not tested	76	No	Yes

All patients received mycophenolate mofetil with corticosteroids in combination with tacrolimus or belatacept.

[a] HLA mismatch is for HLA-A, HLA-B, and HLA-DR.

[b] Preemptive transplantation before the start of renal replacement therapy.

[c] The time in days between transplantation and the biopsy.

[d] Donor-specific antibodies measured with Luminex at time of rejection. eGFR (mL/min per 1.73 m^2) at the time of the biopsy.

ADPKD, autosomal dominant polycystic kidney disease; AMR, antibody-mediated rejection; aTCMR, acute T cell-mediated rejection; ATN, acute tubular necrosis; Bela, belatacept; DGF, delayed graft function; DM, diabetes mellitus; DSA, donor-specific antibodies; eGFR, estimated glomerular filtration rate; GPA, granulomatous polyangiitis; IF/TA, interstitial fibrosis/tubular atrophy; IHC, immunohistochemistry; LR, living related; LUR, living unrelated; MM, mismatch; Tac, tacrolimus; tx, transplantation; VUR, vesicoureeral reflux.

and renal injury, and 7 housekeeping genes. This was based on the panel described in the Banff 2017 report.[5] Probe description and sequences are provided in **Table S2, SDC** (http://links.lww.com/TXD/A157). Gene expression was measured on 120–200 ng of extracted RNA from FFPE biopsies with NanoString. NanoString was previously tested in renal allograft rejection in non human primates.[24,25] Raw gene expression counts of all samples are provided in **Table S3, SDC** (http://links.lww.com/TXD/A158). Background correction, data quality control, normalization of the raw gene expression counts and data analysis was investigated with nSolver Analysis Software (Version 4.0.62). The geNorm algorithm was applied to analyze the stability of the reference genes.[26] Seven reference genes (DDX50, HDAC3, GUSB, POLR2A, OAZ1, UBB, and SDHA) were used for normalization. The parameters for quality control flagging as recommended by the manufacturer were used.[27]

Statistical Analysis

SPSS Version 21 (SPSS Inc., Chicago, IL) was used for IHC analysis. Data are summarized as median and interquartile range. For comparisons between groups, the 2-tailed Mann-Whitney U test was used. A 2-sided *P* value less than .05 was considered significant. For comparison of the 3 groups, Kruskal-Wallis test was used. For gene expression analysis, normalized mRNA expression values were evaluated with the R-based advanced nSolver Advanced Analysis Software (Version 2.0.115). Differential gene expression data are presented as volcano plots and in a summary table showing the top differentially regulated genes. In addition, the data was subjected to unsupervised hierarchical clustering analysis (HCA). The false discovery rate (FDR; Benjamini-Hochberg) method was used to adjust the *P* values for multiple *t*-testing.

RESULTS

Patients

The clinical-pathologic characteristics of the patients are presented in Table 1. Of the 25 patients with rejection, 21 patients had an aTCMR (grade IB to III) and 4 patients had a mixed (aTCMR and active antibody-mediated rejection [AMR]) rejection. The timing of the biopsy and patient age at the time of rejection were not significantly different between the patients treated with belatacept, patients treated with tacrolimus and the negative controls ($P = .42$, and $P = .14$, respectively). The estimated glomerular filtration rate at the time of the acute rejection was similar in patients treated with either tacrolimus or belatacept (median, 26; interquartile range [IQR], 15–35 mL/min per 1.73 m^2; and 28; IQR, 18–41 mL/min per 1.73 m^2; $P = .57$). The median age of the biopsy used for Nanostring was 3.2 years (IQR, 2.3–4.6).

Quality Control of RNA and NanoString

For the gene expression analysis, 7 samples of patients with tacrolimus maintenance therapy, 10 samples of patients with belatacept maintenance therapy, and 6 negative controls (samples without rejection) were analyzed. The mean A_{260}/A_{280} spectrophotometry ratio was 1.88 (standard deviation 0.17). Two samples (1 negative control and 1 sample of a belatacept-treated patient) did not pass the quality control of the nSolver Advanced Analysis Software because of low probe counts and were excluded from further analysis. Of the 209 probes, 16 did not reach the detection threshold (less than double the counts of the median of the negative control) and were excluded from subsequent analysis (**Table S2, SDC;** http://links.lww.com/TXD/A157).

Validation of NanoString

To validate NanoString, it was tested whether NanoString could distinguish between the transcriptome of samples with aTCMR and samples without aTCMR. Unsupervised HCA of the personalized gene panel showed that the samples with aTCMR clustered separately from the negative controls (Figure 1A). However, 1 sample with aTCMR (patient 18) clustered with the negative controls. The clinical data of this patient revealed that he had a slight deterioration of kidney function at the time of the biopsy (serum creatinine rose from 95 to 107 μmol/L). No rejection was diagnosed in the first examination of the biopsy. However, after revision in the setting of the RCT, the biopsy showed an isolated v-lesion and was therefore classified as an aTCMR grade IIA (Banff 2015 classification[23]). After this for-cause biopsy, the kidney function of the patient improved to baseline without antirejection therapy and without adjusting his maintenance immunosuppressive therapy. At present, 45 months after transplantation, the kidney function of this patient is excellent (serum creatinine concentration 92 μmol/L).

Differential gene expression analysis identified a distinct gene signature in biopsies with aTCMR compared to the negative controls (Figure 1B and **Table S4, SDC;** http://links.lww.com/TXD/A159). Comparison of aTCMR and negative controls identified 78 genes with higher expression levels in the aTCMR samples [FDR *P* value <.05 to 1.42e–05; **Table S4; SDC;** http://links.lww.com/TXD/A159], and 1 gene with significantly higher expression in samples without aTCMR (EEF1A1, FDR *P* value 0.047). The most differentially expressed genes (DEGs) were T cell-associated transcripts (CD3, CD8, and CD4; $P < 1.98e{-}04$), γ-interferon-inducible genes (CCL5, CXCL9, CXCL11, CXCL10, TBX21; $P < 1.33e{-}04$), effector genes (GNLY, GZMB, ITGAX; $P < 2.82e{-}03$), macrophage-associated transcripts (SLAMF8, CD86, MS4A7, MRC1, ADAMDEC1; $P < .04$) and injury-repair response-associated transcripts (LCP2, CTSS, FCGR3A, MYBL1, LCN2, and HAVCR1; $P < 4.63e{-}02$). The top 15 DEGs were mainly aTCMR-associated transcripts, denoting an aTCMR profile (Table 2). A 2-dimensional principal component analysis was performed with the top 15 DEGs and showed separate clustering of the samples with acute rejection compared to the negative controls without aTCMR (Figure 1C).

Next, pathway score profiles were compared between samples with aTCMR and negative controls. Seventeen pathways were analyzed (Figure 1D). Each pathway score was a combination of data from 6 to 23 genes (**Table S5, SDC;** http://links.lww.com/TXD/A160). Unsupervised HCA of the 17 pathways showed that the samples with aTCMR clustered separately from the samples without rejection (Figure 1D). Almost all pathway scores were higher in patients with aTCMR, for instance costimulation by the CD28 family, and cytokine signaling.

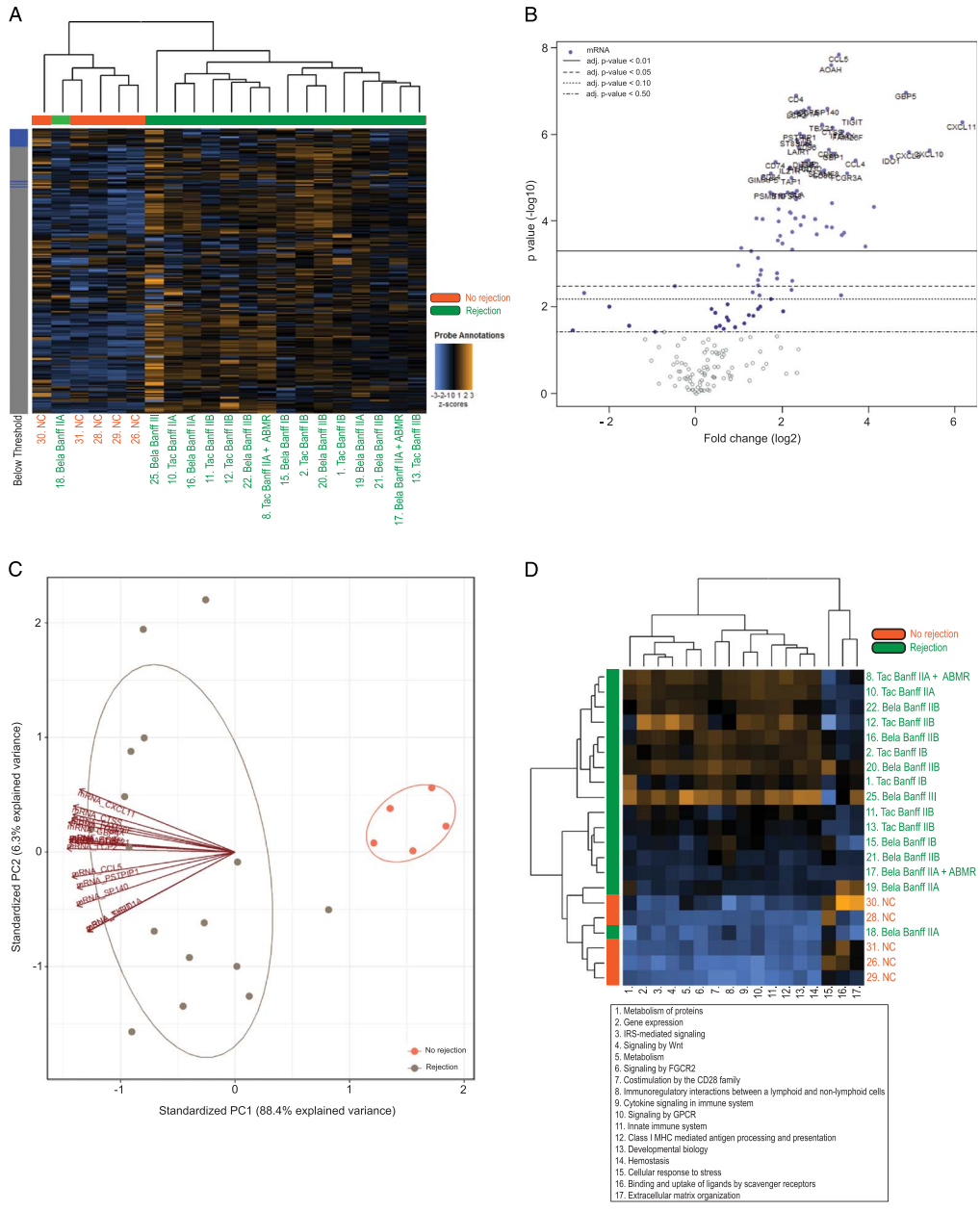

FIGURE 1. A, Heatmap and unsupervised hierarchical cluster analysis of the 209 normalized genes of samples with acute T cell-mediated rejection (aTCMR) and samples without aTCMR (negative controls). Each row represents a probe. Each column represents a biopsy sample. The orange samples are the negative controls. The dark green samples are the samples with acute rejection. The color in each cell reflects the level of expression of the messenger RNA (mRNA), relative to the geometric mean of all the samples (*z* score). Increasing intensities of orange point out higher expression, while increasing intensities of blue indicate lower expression. The degree of relatedness is represented by the dendrogram at the top of the panel. The probe threshold is depicted on the left of the heatmap. Blue cells represent probes that were below the detection threshold (less than double the counts of the median of the negative control). Gray cells represent probes that were above the detection threshold. B, Volcano plot of samples with aTCMR versus patients without aTCMR. The X-axis represents fold change (log2). The Y-axis displays each gene's *P* value (–log10). The horizontal lines indicate various false discovery rate *P* values (FDRPVs). The 40 most statistically significant genes are labeled in the plot. Genes with a positive fold change are higher expressed in the samples with an acute rejection. Genes with a negative fold change are higher expressed in the samples without acute rejection. C, Principal component analysis (PCA) plot of the top 15 "differentially expressed genes (DEGs) in samples with aTCMR and negative controls. PCA samples on the first (X-axis) and second PC plane (Y-axis). The samples without acute rejection are displayed in pink. The samples with acute rejection are displayed in gray. D, Pathway scores of samples with aTCMR and samples without aTCMR. Unsupervised hierarchical cluster analysis and heatmap showing pathway scores. Pathway scores are fit using the first principal component of each gene set's data. Scores are displayed on the same scale via a Z-transformation. Each row represents a sample with patient ID number. Each column represents a pathway. The orange samples are the negative controls. The dark green samples are the samples with rejection. Increasing intensities of orange point out higher pathway scores, while increasing intensities of blue indicate lower pathway scores. The degree of relatedness is represented by the dendrogram at the top of the panel. Each number of the column represents a different pathway (1) metabolism of proteins, (2) gene expression, (3) insulin receptor substrate signaling mediated signaling, (4) signaling by Wnt, (5) metabolism, (6) signaling by fragment C gamma receptor 2 (FGCR2), (7) costimulation by the CD28 family, (8) immunoregulatory interactions between lymphoid and nonlymphoid cells, (9) cytokine signaling in immune system, (10) signaling by G-protein coupled receptor (GPCR), (11) innate immune system, (12) major histocompatibility complex (MHC)-mediated class I antigen processing and presentation, (13) developmental biology, (14) hemostasis, (15) cellular response to stress, (16) binding and uptake of ligands by scavenger receptors, (17) Extracellular matrix organization.

Immunomic Comparison of aTCMR Biopsies Under Belatacept or Tacrolimus Therapy

Immunophenotypical Analysis

Twenty-five biopsies were included in the IHC analysis: 11 biopsies of patients treated with belatacept-based maintenance therapy and 14 patients with tacrolimus-based maintenance therapy. The infiltrates in the cortical area of tacrolimus-treated patients with aTCMR mainly consisted of T cells, monocytes and macrophages (Table 3). Representative IHC stainings of the infiltrate in an aTCMR biopsy of a patient with belatacept maintenance therapy are shown in **Figure S1, SDC** (http://links.lww.com/TXD/A161). The composition of cells in the cortical area was not significantly different for markers of the adaptive immune response (CD3, CD4, CD8, CD20, FoxP3, PD-1 and granzyme B) and for markers of the innate immune response (CD56 and CD68) in both belatacept- and tacrolimus-treated patients (Table 3). Furthermore, no significant difference was seen in the composition of cells in the cortical area between both groups of patients when only aTCMR grade IIA and IIB were analyzed, or when the mixed AR were compared (data not shown).

Gene Expression Analysis

In an unsupervised HCA, using the personalized panel, the gene expression profiles of belatacept-maintenance therapy did not cluster separately from the profiles of tacrolimus maintenance therapy (Figure 2A). Differential gene expression analysis demonstrated no significant difference between the aTCMR samples of patients who received maintenance therapy with either belatacept or tacrolimus (Figure 2B and **Table S6, SDC;** http://links.lww.com/TXD/A162). The top 15 DEGs (although not statistically different) are summarized in Table 4. In a 2-dimensional principal component analysis, no separate clustering was seen between the samples of patients treated with belatacept or tacrolimus maintenance therapy (Figure 2C).

TABLE 3.

IHC analysis of CD3, CD4, CD8, FoxP3, CD20, CD56, CD68, PD-1, and granzyme B

Marker	Treatment	Median[a]	IQR[a]	*P*
CD3	Tacrolimus	7.76	4.93–11.35	.15
	Belatacept	4.18	3.63–8.28	
CD4	Tacrolimus	4.64	1.48–7.84	.85
	Belatacept	4.86	2.84–6.91	
CD8	Tacrolimus	3.23	1.68–5.73	.69
	Belatacept	1.96	1.54–4.25	
FoxP3	Tacrolimus	0.05	0.03–0.22	.58
	Belatacept	0.05	0.02–0.12	
FoxP3/CD4	Tacrolimus	0.009	0.007–0.012	1.00
	Belatacept	0.009	0.006–0.019	
CD20	Tacrolimus	0.43	0.21–2.92	1.00
	Belatacept	1.05	0.29–5.88	
CD56	Tacrolimus	0.05	0.02–0.09	.12
	Belatacept	0.15	0.05–0.39	
CD68	Tacrolimus	10.6	3.6–19.2	.37
	Belatacept	5.6	4.2–10.2	
Granzyme B	Tacrolimus	0.21	0.05–0.47	.81
	Belatacept	0.16	0.08–0.49	
PD-1	Tacrolimus	0.35	0.22–0.70	.12
	Belatacept	0.05	0.02–0.88	

[a] Median (%) and interquartile range (%) of the ratio of positive stained cortex area divided by the total cortex area of CD3, CD4, CD8, CD20, CD56, CD68, granzyme B and PD-1. The ratio of FoxP3/CD3 is calculated by diving the percentage of FoxP3 staining by the percentage of CD4 staining for each section.

IQR, interquartile range; PD-1, programmed cell death protein 1.

Unsupervised HCA of the pathway scores is depicted in Figure 2D. None of the 17 different pathways distinguished between aTCMR occurring under belatacept or tacrolimus maintenance therapy. Surprisingly, the genes that are involved in the CD28 costimulatory pathway were similarly

TABLE 2.

Top 15 of DEGs in patients with an acute rejection compared with patients without an acute rejection

mRNA	FC (log2)	SE (log2)	Lower confidence limit (log2)	Upper confidence limit (log2)	FDRPV[a]	Panel[b]
CCL5	3.32	0.354	2.63	4.02	1.42e–05	Rejection
AOAH	3.14	0.347	2.46	3.82	1.42e–05	TCMR
GBP5	4.87	0.592	3.71	6.03	3.59e–05	TCMR
CD4	2.33	0.287	1.77	2.9	3.59e–05	TCMR
CCR5	2.63	0.338	1.97	3.29	4.18e–05	Rejection
SP140	3.05	0.392	2.28	3.81	4.18e–05	TCMR
SH2D1A	2.5	0.322	1.86	3.13	4.18e–05	TCMR
LCP2	2.34	0.304	1.75	2.94	4.18e–05	TCMR
TIGIT	3.63	0.484	2.68	4.58	5.4e–05	TCMR/Exhaustion
CXCL11	6.17	0.835	4.53	7.81	6.01e–05	AMR
TBX21	2.92	0.397	2.14	3.7	6.01e–05	AMR/exhaustion
CTSS	3.17	0.437	2.31	4.02	6.7e–05	AKI
ITGAX	3.41	0.478	2.47	4.35	7.35e–05	TOLs
FAM26F	3.53	0.498	2.55	4.51	7.35e–05	TCMR
PSTPIP1	2.41	0.341	1.75	3.08	7.35e–05	TCMR

Positive ratio means higher expression in samples with rejection.

[a] FDR *P* value was obtained from the adjusted *P* value of FDR correction by Benjamini-Hochberg method.

[b] Panel in Banff kidney report 2017.[5]

AKI, acute kidney injury; AMR, antibody-mediated rejection; FC, fold change; FDRPV, false discovery rate P value; mRNA, messenger RNA; SE, standard error; TCMR, T cell-mediated rejection, TOLs, tolerance assisted transcripts.

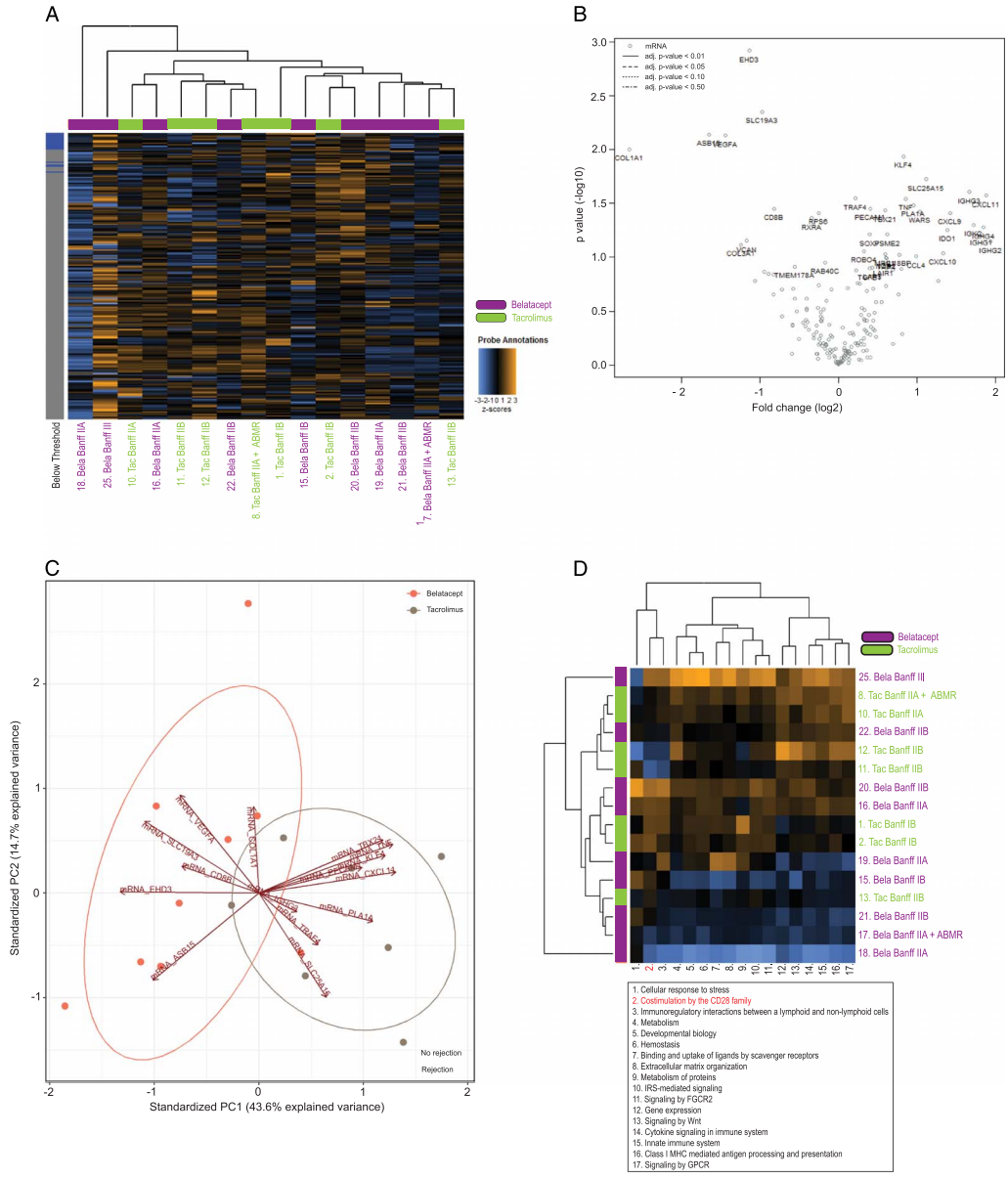

FIGURE 2. A, Heatmap and unsupervised hierarchical cluster analysis of the 209 normalized genes in samples of patients with acute T cell-mediated rejection (aTCMR) treated with belatacept or tacrolimus. Each row represents a probe. Each column represents a biopsy sample. The purple samples are the samples from belatacept-treated patients. The light green samples are the samples from tacrolimus-treated patients. The color in each cell reflects the level of expression of the messenger RNA (mRNA), relative to the geometric mean of all the samples (*z* score). Increasing intensities of orange point out higher expression, while increasing intensities of blue indicate lower expression. The degree of relatedness is represented by the dendrogram at the top of the panel. The probe threshold is depicted on the left of the heatmap. Blue cells represent probes that were below the detection threshold (less than double the counts of the median of the negative control). Gray cells represent probes that were above the detection threshold. B, Volcano plot of samples of patients with aTCMR treated with belatacept versus patients treated with tacrolimus. The X-axis represents fold change (log2). The Y-axis displays each gene's *P* value (–log10). None of the genes was significant different between the 2 groups, therefore no horizontal lines that indicate various false discovery rates *P* values (FDRPVs) are visible. The 40 most statistically significant genes are labeled in the plot. Genes with a positive fold change are higher expressed in the samples of patients treated with tacrolimus. Genes with a negative fold change are higher expressed in the samples of patients treated with belatacept. C, Principal component analysis (PCA) plot of the top 15 differentially expressed genes (DEGs) in samples of patients with aTCMR treated with belatacept or tacrolimus. PCA samples on the first (X-axis) and second PC plane (Y-axis). The samples of patients treated with belatacept are displayed in pink. The samples of patients treated with tacrolimus are displayed in gray. D, Pathway scores of samples of patients with aTCMR treated with belatacept or tacrolimus. Unsupervised hierarchical cluster analysis and heatmap showing pathway scores. Pathway scores are fit using the first principal component of each gene set's data. Scores are displayed on the same scale via a Z-transformation. Each row represents a sample. Each column represents a pathway. The purple samples are the belatacept-treated patients. The light green samples are the samples of patients treated with tacrolimus. Increasing intensities of orange point out higher pathway scores, while increasing intensities of blue indicate lower pathway scores. The degree of relatedness is represented by the dendrogram at the top of the panel. Each number of the column represents a different pathway: (1) Cellular response to stress, (2) Costimulation by the CD28 family, (3) Immunoregulatory interactions between lymphoid and nonlymphoid cells, (4) Metabolism, (5) Developmental biology, (6) Hemostasis, (7) Binding and uptake of ligands by scavenger receptors, (8) Extracellular matrix organization, (9) Metabolism of proteins, (10) Insulin receptor substrate signaling mediated signaling, (11) Signaling by fragment C gamma receptor 2 (FGCR2), (12) Gene expression, (13) Signaling by Wnt, (14) Cytokine signaling in immune system, (15) Innate immune system, (16) Class I major histocompatability complex (MHC) mediated antigen processing and presentation, (17) Signaling by G-protein coupled receptor (GPCR).

TABLE 4.

Top 15 of DEGs in patients with acute rejection treated with belatacept compared with patients treated with tacrolimus

mRNA	FC (log2)	SE (log2)	Lower confidence limit (log2)	Upper confidence limit (log2)	*P*	FDRPV[a]	Panel[b]
EHD3	–1.14	0.28	–1.70	–0.59	.0012	1.00	Glomerulus
SLC19A3	–0.98	0.29	–1.54	–0.41	.0045	1.00	eGFR later
ASB15	–1.65	0.53	–2.68	–0.62	.0073	1.00	GOCAR
VEGFA	–1.44	0.46	–2.35	–0.54	.0074	1.00	Macrophages
COL1A1	–2.67	0.90	–4.43	–0.91	.0099	1.00	CADI progression/matrix
KLF4	0.83	0.29	0.27	1.39	.0116	1.00	AMR
SLC25A15	1.11	0.42	0.29	1.93	.0189	1.00	eGFR later
IGHG3	1.66	0.66	0.36	2.95	.0249	1.00	Plasma cells
CXCL11	1.88	0.76	0.39	3.37	.0269	1.00	AMR
TRAF4	0.21	0.09	0.04	0.38	.0285	1.00	eGFR later
TNF	0.85	0.35	0.17	1.54	.0288	1.00	AMR
PLA1A	0.95	0.40	0.16	1.74	.0328	1.00	AMR
CD8B	–0.83	0.36	–1.52	–0.13	.0355	1.00	TCMR
PECAM1	0.40	0.17	0.06	0.74	.0356	1.00	AMR
TBX21	0.59	0.26	0.09	1.09	.0369	1.00	AMR / Exhaustion

[a] FDRPV was obtained from the adjusted *P* value of FDR correction by Benjamini-Hochberg method.

[b] Panel in Banff kidney report 2017.[5]

AMR, antibody-mediated rejection; CADI, chronic allograft damage index; eGFR, estimated glomerular filtration rate; FC, fold change; FDRPV, false discovery rate *P* value; GOCAR, genomics of chronic allograft rejection; mRNA, messenger RNA; SE, standard error; TCMR, T cell-mediated rejection.

expressed in acute rejection samples of patients treated with either tacrolimus or belatacept (Table 5).

Distinct pretransplant subsets of T cells have been described that may be responsible for triggering belatacept-resistant rejections, namely $CD8^+$ $CD28^-$T cells, $CD4^+CD57^+$programmed death 1 $(PD\text{-}1)^-$ T cells, and $CD8^+CD28^+T_{EMRA}$.[28-31] However, in our RCT, which included the belatacept-treated patients described here, these 3 subsets did not predict acute rejection pretransplantation, at least when measured in peripheral blood.[20] In addition, during acute rejection, the 3 subsets in the blood were not significantly different compared with belatacept-treated patients without acute rejection.[20] In the present study, the intragraft mRNA concentrations of CD4, CD8, CD28, PD-1, and B3GAT1 (alias CD57) were determined and compared between belatacept- and tacrolimus-treated patients with aTCMR (**Table S6, SDC;** http://links.lww.com/TXD/A162). No difference in the expression of these markers was observed between the 2 groups.

DISCUSSION

The integration of immunomics with the conventional histomorphologic examination of renal biopsies will lead to improved classification and a deeper understanding of the pathogenesis of acute rejection.[5] This pilot study shows that with the innovative technique NanoString, it is feasible to derive gene expression data from FFPE kidney transplant biopsies and that it was possible to differentiate biopsies with and without aTCMR. These results were used to support our conclusion that the aTCMR immunomic profiles of patients treated with either tacrolimus or belatacept maintenance therapy were not significantly different.

The Banff 2013 working group recommends the use of molecular diagnostics to define AMR.[32] This includes increased expression analysis of transcripts involved in endothelial injury.[32] The Banff 2017 classification includes more diagnostic and prognostic molecular biomarkers for AMR.[5] However, the Banff 2017 classification does not contain

TABLE 5.

Gene expression ratios of genes involved in the CD28 pathway between patients with an acute rejection treated with belatacept and patients treated with tacrolimus

mRNA	FC (log2)	SE (log2)	Lower confidence limit (log2)	Upper confidence limit (log2)	*P*	FDRPV[a]
BTLA	–0.15	0.52	–1.16	0.87	.77	1.00
CD274	0.47	0.41	–0.32	1.27	.24	1.00
CD28	–0.42	0.46	–1.32	0.49	.37	1.00
CD3D	–0.41	0.38	–1.16	0.35	.29	1.00
CD4	0.25	0.30	–0.33	0.83	.40	1.00
CD86	0.05	0.49	–0.91	1.02	.92	1.00
CTLA4	–0.59	0.73	–2.01	0.84	.42	1.00
ICOS	–0.17	0.45	–1.05	0.71	.71	1.00
PDCD1	–0.42	0.53	–1.46	0.62	.43	1.00
PDCD1LG2	0.03	0.41	–0.77	0.83	.94	1.00

[a] FDRPV was obtained from the adjusted *P* value of FDR correction by Benjamini-Hochberg method.

FC, fold change; FDRPV, false discovery rate *P* value; mRNA, messenger RNA; SE, standard error.

recommendations on the implementation of molecular diagnostics for the diagnosis of aTCMR. This may be useful in differential diagnostic dilemmas, such as borderline rejection or isolated v-lesions.

NanoString is a high-throughput gene expression quantification system that delivers direct multiplexed measurements of gene expression through digital readouts of mRNA transcripts. Formalin-fixation can cause cross-linkage of nucleic acids to proteins, which can lead to inhibition of reverse transcriptase. The advantage of the NanoString over other high-throughput techniques like real-time polymerase chain reaction and microarray, is that it does not require a reverse transcriptase step.[9,33] NanoString is suitable for clinical purposes because it is fast and has minimal hands-on time. Furthermore, the gene expression analysis can be performed in the same formalin fixed paraffin tissue that is used for conventional histopathologic examination. It has been accepted into international treatment guidelines as a prognostic assay for breast cancer.[34]

Here, the allograft transcriptome of aTCMR biopsies showed a significantly higher expression of 78 genes compared with the biopsies without aTCMR. The top pathogenesis-based transcripts were mostly T cell-associated, γ-interferon inducible and effector cell, and injury-repair response-associated transcripts denoting an aTCMR profile.[35]

This is the first study that compared the immunomics of biopsies with aTCMR of patients treated with either tacrolimus or belatacept. A better understanding of the pathogenesis of costimulation blockade resistant rejections could lead to a more personalized approach of belatacept-based treatment in kidney transplant recipients. Besides, because molecular diagnostics of rejection biopsies are increasingly used in combination with conventional histomorphologic examination,[5] it is important to know whether the gene signature of rejection biopsies is dependent of the maintenance immunosuppressive therapy.

In this pilot study with a small sample size, the transcriptome of patients treated with either 1 of the 2 immunosuppressive regimens showed no distinct gene signature, including the genes involved in the CD28 costimulatory pathway. In addition, immunophenotypical analysis of the classic immune markers of the innate and adaptive immune system was not significantly different between the 2 maintenance therapies. Furthermore, we could not confirm that the previously described T-cell subsets ($CD8^+CD28^-$ T cells, $CD4^+CD57^+PD\text{-}1^-$ T cells, and $CD8^+CD28^+T_{EMRA}$[21,28,29]) were associated with belatacept-resistant rejections, neither in the peripheral blood[20] nor in the renal allograft (in this study).

One study analyzed biopsies with aTCMR of patients treated with belatacept or cyclosporine A (CsA) and compared the ratio of $FoxP3^+$ cells among T cells with IHC.[36] This ratio was significantly elevated in acute rejection biopsies of belatacept-treated patients compared to CsA-treated patients (17.99% versus 6.45%, respectively, $P = .044$).[36] Here, no difference was found in the ratio of $FoxP3^+$ cells among $CD4^+$ T cells between aTCMR biopsies of belatacept- and tacrolimus-treated patients. Besides, the intragraft mRNA level of $FoxP3^+$ was similar between the 2 groups.

No studies have compared the immunomics of biopsies without aTCMR of patients treated with belatacept or tacrolimus. However, several studies compared intragraft gene expression and IHC of biopsies without rejection of patients treated with belatacept or cyclosporine. Two studies compared the intragraft gene expression of 12-month protocol biopsies without rejection of patients treated with belatacept or CsA.[37,38] Grimbert et al[37] found that the expression of FoxP3 was less in biopsies of patients treated with belatacept compared with CsA. No differences were found in granzyme B expression or the intragraft expression of genes associated with Th1 (IFNγ, Tbet), Th2 (GATA3), and Th17 (RORγt, IL-17) cells. Vitalone et al[38] compared the intragraft gene expression of 4451 genes of preimplantation biopsies with 12-month protocol biopsies of patients treated with belatacept or CsA. The biopsies of CsA-treated patients showed higher expression of genes associated with fibrosis, early tubulointerstitial damage and CsA-related toxicity. The biopsies of patients treated with belatacept showed enrichment of genes associated with NK cells and monocytes, progressive immune injury and wound healing.[38] Furuzawa-Carballeda et al[39] analyzed the 1-year protocol biopsies (without rejection) with IHC under belatacept or CsA-maintenance treatment and observed that biopsies of belatacept-treated patients showed less senescence and a more immunomodulatory phenotype.

The explanation for the absence of a difference in the immunomics of aTCMR biopsies of patients treated with tacrolimus or belatacept could be that the aTCMR as seen in biopsies is a shared final common pathway. This phenomenon was previously named the "immunologic constant of rejection."[40,41] This hypothesis is based on the observation that different immune-mediated tissue destruction processes share the same final molecular mechanism, like allograft rejection, cancer, autoimmunity, and infections and includes activation of γ-interferon–regulated genes, recruitment of cytotoxic cells by chemokine ligands and activation of immune effector function genes.[40,41]

We recognize the limitations associated with this pilot study, most notably the small number of patients. This could have influenced the power of this study. However, to date, our RCT is the largest to have compared belatacept to tacrolimus maintenance treatment. Furthermore, we feel that studies on the immunomics of belatacept-resistant rejection with more statistical power are unlikely to become available anytime soon since the treatment of new patients with belatacept is currently very difficult because of a worldwide shortage of the drug.[42] Because of the limited sample size, no correlation between the IHC stainings, Banff grade and gene transcripts could be investigated. Furthermore, the scope of this study was to analyze the immunomics of tacrolimus- and belatacept-treated patients with acute rejections and not to study the gene expression profiles of different types of rejection. Therefore, we studied aTCMR only because AMR did not occur in our belatacept RCT which compared belatacept and tacrolimus.

Additionally, we have used the NanoString technique to measure the expression of a limited number of genes instead of using an untargeted approach, thereby excluding other possible differentiating biomarkers. The use of an untargeted genomic approach on the AR biopsies could possibly identify new genes and pathways that we did not analyze with the gene panel used in our study. However, we believe that most genes involved in aTCMR were included as they were derived from the panel presented in the Banff 2017 report.[5] Lastly, more biopsies of the tacrolimus-treated patients used for Nanostring were taken earlier after transplantation than the biopsies of the belatacept-treated patients and the

negative controls. This can be relevant because genes involved in the injury-repair response and inflammation could be affected by the transplant surgery. However, the timing of the acute rejection was not different between the 3 groups.

In summary, no differences were found in the immunomic profiles of aTCMR biopsies of patients treated with tacrolimus- or belatacept-based maintenance therapy, suggesting that clinically diagnosed rejection is a final common pathway of allo-recognition which is independent of the specific immunosuppressive regimen (tacrolimus or belatacept) under which it occurs. Follow-up studies with larger patient numbers are required to confirm our findings when belatacept is widely available again.[42]

ACKNOWLEDGMENTS

The authors thank Jan H. von der Thüsen for assistance with classification of the kidney biopsies.

REFERENCES

1. Loupy A, Lefaucheur C, Vernerey D, et al. Molecular microscope strategy to improve risk stratification in early antibody-mediated kidney allograft rejection. *J Am Soc Nephrol*. 2014;25:2267–2277.
2. Adam B, Afzali B, Dominy KM, et al. Multiplexed color-coded probe-based gene expression assessment for clinical molecular diagnostics in formalin-fixed paraffin-embedded human renal allograft tissue. *Clin Transplant*. 2016;30:295–305.
3. Adam B, Mengel M. Molecular nephropathology: ready for prime time? *Am J Physiol Renal Physiol*. 2015;309:F185–F188.
4. Venner JM, Famulski KS, Badr D, et al. Molecular landscape of T cell-mediated rejection in human kidney transplants: prominence of CTLA4 and PD ligands. *Am J Transplant*. 2014;14:2565–2576.
5. Haas M, Loupy A, Lefaucheur C, et al. The Banff 2017 kidney meeting report: revised diagnostic criteria for chronic active T cell-mediated rejection, antibody-mediated rejection, and prospects for integrative endpoints for next-generation clinical trials. *Am J Transplant*. 2018;18:293–307.
6. Schinstock CA, Sapir-Pichhadze R, Naesens M, et al. Banff survey on antibody-mediated rejection clinical practices in kidney transplantation: diagnostic misinterpretation has potential therapeutic implications. [published online June 23, 2018]. *Am J Transplant*. 2018; doi:10.1111/ajt.14979.
7. Zhang P, Lehmann BD, Shyr Y, et al. The utilization of formalin fixed-paraffin-embedded specimens in high throughput genomic studies. *Int J Genomics*. 2017;2017:1926304.
8. Geiss GK, Bumgarner RE, Birditt B, et al. Direct multiplexed measurement of gene expression with color-coded probe pairs. *Nat Biotechnol*. 2008; 26:317–325.
9. Sigdel TK, Nguyen M, Dobi D, et al. Targeted transcriptional profiling of kidney transplant biopsies. *Kidney Int Rep*. 2018;3:722–731.
10. Nankivell BJ, Borrows RJ, Fung CL, et al. The natural history of chronic allograft nephropathy. *N Engl J Med*. 2003;349:2326–2333.
11. Nankivell BJ, P'Ng CH, O'Connell PJ, et al. Calcineurin inhibitor nephrotoxicity through the lens of longitudinal histology: comparison of cyclosporine and Tacrolimus eras. *Transplantation*. 2016;100:1723–1731.
12. Larsen CP, Pearson TC, Adams AB, et al. Rational development of LEA29Y (belatacept), a high-affinity variant of CTLA4-Ig with potent immunosuppressive properties. *Am J Transplant*. 2005;5:443–453.
13. Archdeacon P, Dixon C, Belen O, et al. Summary of the US FDA approval of belatacept. *Am J Transplant*. 2012;12:554–562.
14. de Graav GN, Bergan S, Baan CC, et al. Therapeutic drug monitoring of belatacept in kidney transplantation. *Ther Drug Monit*. 2015;37:560–567.
15. Vincenti F, Charpentier B, Vanrenterghem Y, et al. A phase III study of belatacept-based immunosuppression regimens versus cyclosporine in renal transplant recipients (BENEFIT study). *Am J Transplant*. 2010;10: 535–546.
16. Durrbach A, Pestana JM, Florman S, et al. Long-term outcomes in belatacept- versus cyclosporine-treated recipients of extended criteria donor kidneys: final results from BENEFIT-EXT, a phase III randomized study. *Am J Transplant*. 2016;16:3192–3201.
17. Durrbach A, Pestana JM, Pearson T, et al. A phase III study of belatacept versus cyclosporine in kidney transplants from extended criteria donors (BENEFIT-EXT study). *Am J Transplant*. 2010;10:547–557.
18. Vincenti F, Rostaing L, Grinyo J, et al. Belatacept and long-term outcomes in kidney transplantation. *N Engl J Med*. 2016;374:333–343.
19. Vincenti F, Larsen CP, Alberu J, et al. Three-year outcomes from BENEFIT, a randomized, active-controlled, parallel-group study in adult kidney transplant recipients. *Am J Transplant*. 2012;12:210–217.
20. de Graav GN, Baan CC, Clahsen-van Groningen MC, et al. A randomized controlled clinical trial comparing Belatacept with Tacrolimus after de novo kidney transplantation. *Transplantation*. 2017;101:2571–2581.
21. de Graav GN, Hesselink DA, Dieterich M, et al. An acute cellular rejection with detrimental outcome occurring under Belatacept-based immunosuppressive therapy: an immunological analysis. *Transplantation*. 2016;100:1111–1119.
22. Shuker N, Bouamar R, van Schaik RH, et al. A randomized controlled trial comparing the efficacy of Cyp3a5 genotype-based with body-weight-based tacrolimus dosing after living donor kidney transplantation. *Am J Transplant*. 2016;16:2085–2096.
23. Loupy A, Haas M, Solez K, et al. The Banff 2015 kidney meeting report: current challenges in rejection classification and prospects for adopting molecular pathology. *Am J Transplant*. 2017;17:28–41.
24. Smith RN, Matsunami M, Adam BA, et al. RNA expression profiling of non-human primate renal allograft rejection identifies tolerance. *Am J Transplant*. 2018;18:1328–1339.
25. Smith RN, Adam BA, Rosales IA, et al. RNA expression profiling of renal allografts in a nonhuman primate identifies variation in NK and endothelial gene expression. *Am J Transplant*. 2018;18:1340–1350.
26. Vandesompele J, De Preter K, Pattyn F, et al. Accurate normalization of real-time quantitative RT-PCR data by geometric averaging of multiple internal control genes. *Genome Biol*. 2002;3:RESEARCH0034.
27. nanoString. nSolver 4.0 analysis software user manual. Available at https://www.nanostring.com/application/files/2915/1060/0919/nSolver_4.0_User_Manual.pdf. Accessed on 14 December 2017.
28. Espinosa J, Herr F, Tharp G, et al. CD57(+) CD4 T cells underlie belatacept-resistant allograft rejection. *Am J Transplant*. 2016;16:1102–1112.
29. Mathews DV, Wakwe WC, Kim SC, et al. Belatacept-resistant rejection is associated with CD28+ memory CD8 T cells. *Am J Transplant*. 2017;17:2285–2299.
30. Lo DJ, Weaver TA, Stempora L, et al. Selective targeting of human alloresponsive CD8+ effector memory T cells based on CD2 expression. *Am J Transplant*. 2011;11:22–33.
31. Xu H, Perez SD, Cheeseman J, et al. The allo- and viral-specific immunosuppressive effect of belatacept, but not tacrolimus, attenuates with progressive T cell maturation. *Am J Transplant*. 2014;14:319–332.
32. Haas M, Sis B, Racusen LC, et al. Banff 2013 meeting report: inclusion of c4d-negative antibody-mediated rejection and antibody-associated arterial lesions. *Am J Transplant*. 2014;14:272–283.
33. Bustin S, Dhillon HS, Kirvell S, et al. Variability of the reverse transcription step: practical implications. *Clin Chem*. 2015;61:202–212.
34. nanoString. Prosigna. Available at https://www.nanostring.com/diagnostics/prosigna. Accessed on 6 april 2018.
35. Halloran PF, Famulski K, Reeve J. The molecular phenotypes of rejection in kidney transplant biopsies. *Curr Opin Organ Transplant*. 2015;20:359–367.
36. Bluestone JA, Liu W, Yabu JM, et al. The effect of costimulatory and interleukin 2 receptor blockade on regulatory T cells in renal transplantation. *Am J Transplant*. 2008;8:2086–2096.
37. Grimbert P, Audard V, Diet C, et al. T-cell phenotype in protocol renal biopsy from transplant recipients treated with belatacept-mediated costimulatory blockade. *Nephrol Dial Transplant*. 2011;26:1087–1093.
38. Vitalone MJ, Ganguly B, Hsieh S, et al. Transcriptional profiling of belatacept and calcineurin inhibitor therapy in renal allograft recipients. *Am J Transplant*. 2014;14:1912–1921.
39. Furuzawa-Carballeda J, Lima G, Alberú J, et al. Infiltrating cellular pattern in kidney graft biopsies translates into forkhead box protein 3 up-regulation and p16INK4α senescence protein down-regulation in patients treated with belatacept compared to cyclosporin a. *Clin Exp Immunol*. 2012;167:330–337.
40. Wang E, Worschech A, Marincola FM. The immunologic constant of rejection. *Trends Immunol*. 2008;29:256–262.
41. Spivey TL, Uccellini L, Ascierto ML, et al. Gene expression profiling in acute allograft rejection: challenging the immunologic constant of rejection hypothesis. *J Transl Med*. 2011;9:174.
42. Gabardi S, van Gelder T. Causes and consequences of the worldwide belatacept shortage. *Transplantation*. 2017;101:1520–1521.